Thermodynamics of the Al₂O₃–Al₄C₃ system III. Equilibrium vapour pressures and activation energies for volatilisation

J.-M. Lihrmann*

LIMHP, UPR CNRS 1311, Avenue J.-B. Clément, 93430 Villetaneuse, France

Abstract

The present paper addresses the vapour phase in equilibrium with the compounds of the stable Al_2O_3–Al_4C_3 system, between 25 °C and 1827 °C. The volatilisation of each of them into any of five gaseous species referred to as $[Al_xO_y]$, is described in terms of an activation energy and a pre-exponential term; for Al_2O_3, also sublimation is modelled on the basis of rare vapourization data. At least up to 1300 °C, the relative importance of the various $[Al_xO_y]$ derives from the activation energies necessary to form them; above 1300 °C, both activation energy and pre-exponential terms are influential. Activation energies increase with increasing ratio y/x in $[Al_xO_y]$, from approximately 365 kJ mol⁻¹ for $[Al]$ to about 900 kJ mol⁻¹ for $[AlO_2]$; the effects of temperature and mole fraction Al_2O_3 are investigated. Up to almost 1807 °C, $[Al]$ is the predominant species regardless of carbon monoxide pressure, and thus the most likely intermediate in processes involving vapour phase reactions. Solid–vapour equilibria are illustrated in a volatility diagram at 1787 °C.

© 2007 Elsevier Ltd. All rights reserved.

Keywords: Al_2O_3; Carbides; Chemical properties; Thermal properties; Vapour pressures

1. Introduction

Full understanding of the Al_2O_3–Al_4C_3 system requires description of all condensed phases in stable or metastable equilibrium states, and also of the vapour phase, which may consist of several species differing in composition and partial pressures. The vapour phase is of prime importance in materials' processing: during sintering of ceramics it is involved in weight losses through volatilisation, and/or in vapour phase transfer reactions leading to grain coarsening that prevents densification[1]; in metallurgical processes it creates the oxidation or reducing potential which makes a chemical reaction occur when diffusion and overall kinetics are favourable enough.

Unlike Al_2O_3, Al carbide and oxycarbides are lesser-known materials. The crystal structures of Al_4C_3 and Al_4O_4C are described in Refs. [2–4] and well recognized. The situation with Al_2OC is less precise because, although it was shown in Parts I and II (Refs. [5,6]) that this oxycarbide is stable only above 1710.038 °C, its lattice parameters[7–11] and even some thermodynamic properties are often indicated at room temperature. This is mainly due to the similarity of Al_2OC with other würtzite compounds,[12] especially AlN, of which a minor amount as a solute suffices to prevent eutectoid decomposition at 1710 °C, i.e. stabilizes the compound as a $(Al_2OC)_{1-x}$–$(AlN)_x$ solid solution; another possible explanation is the out-of-equilibrium cooling of the compound following its high temperature formation, which is also a stabilising route. The occurrence of Al_2OC in a metastable Al_2O_3–Al_4C_3 system, and the stabilizing influence of AlN have both been demonstrated[13] and may be further analysed in future supplementary papers, in view of the current thermodynamic knowledge and other more recent data.

Earlier experiments[14] performed in a high temperature, graphite tube electrical furnace showed that alumina and carbon reacted in a way determined by temperature. At extremely high values, volatilisation, within a few minutes, of all Al_2O_3 and of some graphite was observed, followed by condensation, on each side outside the heating element, of a crystalline felting

* Correspondence address: 66 bis rue des Pâtis, 95520 Osny, France.
Tel.: +33 1 34 43 54 06.
E-mail address: j.mlihrmann@free.fr.

of carbon and alumina, and minor amounts of metallic Al on yet colder parts of the equipment. At lower values, however still above 2000 °C, mixtures of Al_2O_3 and starch within a graphite tube reacted to form a substantial Al deposit, enclosing lamellae of aluminium carbide and covered by a thin carbon layer resulting from the condensation of the vapour filling the tube. Later, mass spectrometer studies[15] of Al_2O_3 identified Al, Al_2O, AlO and Al_2O_2 as the main Al-containing gaseous species; the additional AlO_2 (g) was included here due to previous theoretical foundations[16] and calculations.[17] All these species are mentioned in a number of recent thermodynamic analyses and investigations of the Al_2O_3–Al_4C_3, alumina–graphite or Al_2O_3–SiC systems, e.g. Refs. [18–22] with sometimes opposite conclusions about the equilibrium vapour phase. This can be witnessed for the Al_2O_3–Al_4C_3 system, where one study found p_{CO_2}, p_{O_2}, p_{Al_2O}, and p_{AlO} values to be negligible compared to the p_{Al} and p_{CO} values,[18] while another insisted that appreciable amounts of Al_2O were present in the vapour.[19] In addition, solid Al_2O_3[23] and oxycarbides Al_4O_4C and Al_2OC[24] have been reported to have high vapour pressures above 1700 °C, without precise values being mentioned. Based on thermodynamic data listed[5] in Part I, the present paper attempts to clarify the situation and describes the volatilisation of the stable compounds of the Al_2O_3–Al_4C_3 system into various Al-containing gaseous species, up to 1826.85 °C; for alumina, sublimation is included in the development, following estimation of a probable phase equilibrium diagram for this component.

Determining the pressure of any gaseous species formed by volatilisation from a solid compound makes use of the well-known temperature-dependent equilibrium constant K_p, such that $Ln\,K_p = -\Delta_r G^\circ / RT$, where R is the perfect-gas constant, and is shown to develop into an Arrhenius-type equation which includes a pre-exponential term and an activation energy for volatilisation. The magnitudes of the different partial pressures depend primarily on the latter, so that in most situations the major gas species is Al, closely followed at higher temperatures by Al_2O; AlO and Al_2O_2 are less important by several orders of magnitude, and so is AlO_2 relative to the latter two. More precisely, it is shown that below 1806.65 °C, Al is the major vapour species whereas above, Al_2O is more important, yet only over quite limited ranges of carbon monoxide pressures; the Al_2O_3 vapour pressure only slightly exceeds 1.1×10^{-5} atm at 1827 °C.

The ease to graphically represent any solid–gas system at equilibrium increases when the number of degrees of freedom, or so-called variance v, diminishes, so that univariant ($v = 1$) and divariant ($v = 2$) reactions are most convenient. In this respect, several forms of essentially equivalent graphs exist, including reducing potential[25] and volatility[26] diagrams. Here the second form is more suitable due to the variety of gaseous species, and is illustrated at 1786.85 °C.

2. Rationale

Compounds and vapour species entering the study are represented in Fig. 1 within the three – independent – constituent system Al–C–$(1/2)O_2$·Al_2O_3, Al_4C_3, Al_4O_4C, Al_2OC and C
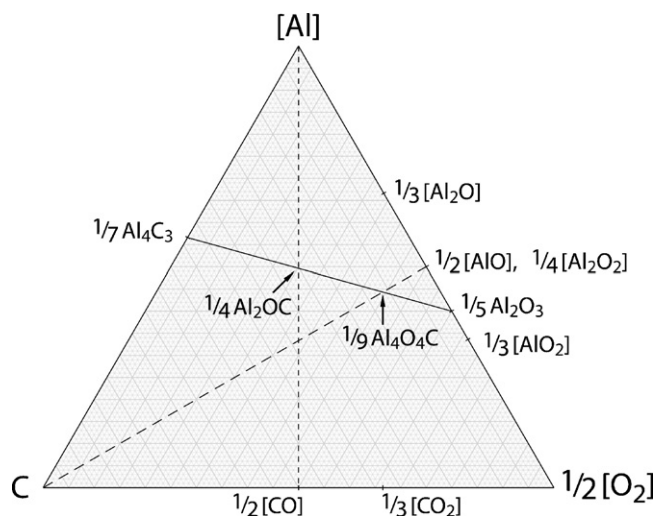

Fig. 1. Unit solid and gaseous species dealt with in this paper, in unit ternary system Al(g)–C(s)–(1/2)O₂(g).

(graphite) are solid at all temperatures between 25 °C and 1827 °C, and no specific mark is used to specify their physical state; for distinction the gaseous species are written with brackets, e.g. [Al]. Advantageous sets of independent intensive parameters making it possible to quantify the various equilibria include temperature as an obvious prominent choice, and partial pressure of either carbon monoxide, oxygen or carbon dioxide, because thermodynamic laws of equilibria are such that the partial pressure of any Al-containing species, $[Al_xO_y]$, can be expressed as a function of temperature and either one of these three connected parameters (it is straightforward that

Table 1
Standard Gibbs free energies of formation, in S.I. units (J, mole, K)

[CO]	
25–660 °C	$-110299.5046 - 90.1966T$
660–1227 °C	$-113462.3097 - 86.8694T$
1227–1827 °C	$-117172.0234 - 84.4077T$
[Al]	
25–660 °C	$324997.8783 - 132.6074T$
660–1227 °C	$307588.7524 - 113.8454T$
1227–1827 °C	$301565.0874 - 109.8375T$
[Al₂O]	
25–660 °C	$-135823.6977 - 88.1883T$
660–1227 °C	$-171366.8773 - 49.5051T$
1227–1827 °C	$-182198.5560 - 42.2958T$
[AlO]	
25–660 °C	$80750.0000 - 80.3333T$
660–1227 °C	$63138.1539 - 61.6997T$
1227–1827 °C	$58313.3046 - 58.4580T$
[Al₂O₂]	
25–660 °C	$-410600.0000 + 8.6667T$
660–1227 °C	$-444488.2362 + 45.7347T$
1227–1827 °C	$-452545.6240 + 51.0986T$
[AlO₂]	
25–660 °C	$-184997.6520 - 9.8160T$
660–1227 °C	$-199544.3242 + 5.8026T$
1227–1827 °C	$-203404.8611 + 8.3665T$

Table 2
Functions $\log p_{[Al_xO_y]} = (a/b)\log p_{[CO]} + (-B + AT)/[b(Ln_{10}) \times 8.314T]$, in stable system $Al_2O_3 - Al_4C_3$

Compound	$[Al_xO_y]$	a	b	B		A	
				660–1227 °C	1227–1827 °C	660–1227 °C	1227–1827 °C
	$[Al]$	−3	2	1,966,454.8282	1,935,210.4339	818.5545	797.7805
	$[Al_2O]$	−2	1	1,293,372.7558	1,267,053.7265	553.4994	535.9936
Al_2O_3	$[AlO]$	−1	2	1,704,478.2506	1,683,050.9151	540.5243	526.2061
	$[Al_2O_2]$	−1	1	1,133,713.7066	1,113,878.6819	371.3902	358.1915
	$[AlO_2]$	1	2	1,406,037.9138	1,393,958.6305	231.7809	223.7417
	$[Al]$	0	4	1,493,794.3320	1,468,434.2939	555.9659	539.2002
	$[Al_2O]$	2	2	147,630.1872	132,120.8791	25.8557	15.6264
Al_4C_3	$[AlO]$	4	4	969,954.1768	964,115.2563	−0.0945	−3.9486
	$[Al_2O_2]$	4	2	−171,687.9112	−174,229.2101	−338.3627	−339.9778
	$[AlO_2]$	8	4	372,960.5032	385,930.6871	−617.5813	−608.8774
	$[Al]$	−4	4	3,130,971.1902	3,080,858.4003	1276.7279	1243.4407
	$[Al_2O]$	−2	2	1,784,807.0454	1,744,544.9855	746.6117	719.8669
Al_4O_4C	$[AlO]$	0	4	2,607,018.0350	2,576,539.3627	720.6675	700.2919
	$[Al_2O_2]$	0	2	1,465,488.9470	1,438,194.8963	382.3993	364.2627
	$[AlO_2]$	4	4	2,010,137.3614	1,998,354.7935	103.1807	95.3631

Compound	$[Al_xO_y]$	a	b	B (T'–1827 °C)	A (T'–1827 °C)
	$[Al]$	−1	2	1,100,999.8644	427.3593
	$[Al_2O]$	0	1	432,843.1570	165.5724
Al_2OC	$[AlO]$	1	2	848,840.3456	155.7849
	$[Al_2O_2]$	1	1	279,668.1124	−12.2297
	$[AlO_2]$	3	2	559,748.0610	−146.679

to any given carbon monoxide pressure there correspond both an $[O_2]$ pressure, via the reaction $C + (1/2)[O_2] = [CO]$, and a $[CO_2]$ pressure, via the reaction $C + [CO_2] = 2[CO]$, at any given temperature). The relevant thermochemical functions needed to quantify the various equilibria have been calculated[5] in Part I; for convenience, their linear counter-parts, which have been shown to provide adequate precision, have been utilized in the following calculations. The additional standard Gibbs free energies of formation, listed in Table 1, were obtained from Janaf[17]; also for convenience, all pressures are expressed in atmospheres (atm). Not mentioned in Table 1 is the standard Gibbs free energies of formation of $[CO_2]$, for which a constant value, −396,400 J mol^{-1}, was assumed in the temperature interval 1227–1827 °C, in excellent agreement with Ref. [17].

3. Results

The aforesaid expressions of $\log p_{[Al_xO_y]}$ are listed in Table 2 for the temperatures above the melting point of aluminium (660 °C); below, equilibrium vapour pressures can be shown

to be much less significant. The range of carbon monoxide pressures in equilibrium with each stable compound is imposed by the reactions of Table 3, in such a manner that, for Al_4C_3, its upper limit is $p_{[CO],d_1}$, $p_{[CO],d_2}$ or $p_{[CO],c}$, while for Al_2O_3 its lower limit is $p_{[CO],a_1}$ or $p_{[CO],a_2}$, depending on temperature. For Al_2OC this range is limited by reactions (b) and (c), whereas for Al_4O_4C it is established either by $p_{[CO],a_1}$ and $p_{[CO],d_1}$, or by $p_{[CO],a_2}$, $p_{[CO],d_2}$ and $p_{[CO],b}$ according to whether the temperature range is 660–1227 °C, 1227–T' or T'–1827 °C, with $T' = 1710.038$ °C. Thus, substituting $\log p_{[CO]}$ of Table 2 with the appropriate expression of Table 3 makes it possible to determine, as functions of temperature, the pressures of all Al-containing species in equilibrium with the various stable compounds of the $Al_2O_3 - Al_4C_3$ system, for the particular carbon monoxide pressures of the univariant reactions of Table 3. Table 4 indicates these at three temperatures, 786.85 °C, 1286.85 °C and 1786.85 °C, and Fig. 2 depicts at 1786.85 °C the equilibrium pressures of Al-containing species, as defined by Tables 2 and 3, in the range of carbon monoxide pressures between 0.0631 atm and 0.2512 atm.

Table 3
Functions $\log p_{[CO],i} = (-D + CT)/[2(Ln_{10}) \times 8.314T]$, for the univariant reactions of stable system $Al_2O_3 - Al_4C_3$

Reaction	Temperature range (°C)	$p_{[CO],i}$ (atm)	D	C
$(a_1) 2Al_2O_3 + 3C = Al_4O_4C + 2[CO]$	660–1227	$p_{[CO],a_1}$	801,938.4662	360.3751
$(a_2) 2Al_2O_3 + 3C = Al_4O_4C + 2[CO]$	1227–1827	$p_{[CO],a_2}$	789,562.4675	352.1203
$(b) Al_4O_4C + 3C = 2Al_2OC + 2[CO]$	T'–1827	$p_{[CO],b}$	878,858.6715	388.7221
$(c) 2Al_2OC + 3C = Al_4C_3 + 2[CO]$	T'–1827	$p_{[CO],c}$	733,565.4349	315.5184
$(d_1) Al_4O_4C + 6C = Al_4C_3 + 4[CO]$	660–1227	$p_{[CO],d_1}$	818,588.4291	360.3810
$(d_2) Al_4O_4C + 6C = Al_4C_3 + 4[CO]$	1227–T'	$p_{[CO],d_2}$	806,212.0532	352.12025

Table 4
Decimal logarithms of $p_{[Al_xO_y]}$ at univariant reactions (Al_4C_3, Al_2O_3) or in entire range of equilibrium (Al_2OC, Al_4O_4C)

| Al_xO_y	786.85 °C			1286.85 °C			1786.85 °C			
	Al_4C_3	Al_4O_4C	Al_2O_3	Al_4C_3	Al_4O_4C	Al_2O_3	Al_4C_3	Al_2OC	Al_4O_4C	Al_2O_3
[Al]	−11.1430	−11.1430 to −11.5531	−11.5530	−5.2511	−5.2511 to −5.5299	−5.5299	−2.2675	−2.3024 to −2.2675	−2.3024 to −2.4786	−2.4786
[Al₂O]	−13.7197	−13.7198 to −14.1299	−14.1296	−6.1051	−6.1051 to −6.3839	−6.3839	−2.3269	−2.3269	−2.3269 to −2.5031	−2.5031
[AlO]	−22.7084	−22.7070	−22.7069	−12.4236	−12.4236	−12.4236	−7.2234	−7.1885 to −7.2234	−7.1885	−7.1885
[Al₂O₂]	−26.1219	−26.1219	−26.1217	−14.5650	−14.5650	−14.5650	−8.7904	−8.7206 to −8.7904	−8.7206	−8.7206
[AlO₂]	−34.1747	−34.1747 to −33.7646	−33.7645	−19.7846	−19.7846 to −19.5058	−19.5058	−12.5178	−12.5178 to −12.4131	−12.4131 to −12.2369	−12.2369
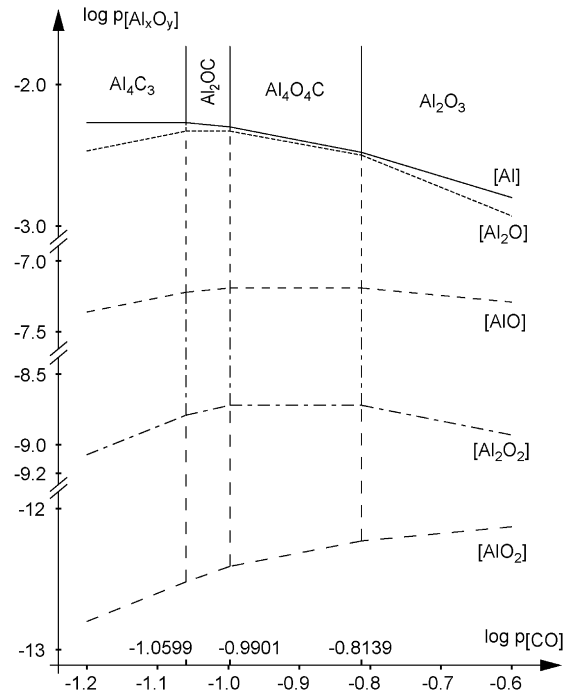
Fig. 2. Volatility diagram at 1786.85 °C.

To know how these compare with the Al₂O₃ vapour pressure, it is necessary to question the phase diagram of this compound. Assuming that gaseous Al₂O₃ is a perfect gas with a mole volume much larger than that of alumina, the solid–vapour equilibrium can be described by the well known Clausius–Clapeyron equation which makes use of the latent heat of sublimation; this not-readily known property rigorously amounts to the sum of its more accessible melting and vapourization counterparts, at the triple point of the phase diagram. Based on a normal boiling point[17,27] of 2976.85 °C and a vapour pressure[27] of $(760)^{-1}$ atm at 2158 °C, the liquid–vapour equilibrium curve follows Eq. (1) below:

$$\text{Ln } p_{[Al_2O_3]} = 19.6942 - \frac{532147}{RT} \tag{1}$$

Over a wide temperature range, the solid–liquid equilibrium curve is a steep straight line, the gradient of which can be determined at the (normal) melting point, 2054 °C,[28] using the Clapeyron equation. The latent heat[28] of fusion is 111,100 J mol⁻¹ and the calculated solid density at that temperature is 3.7134 g cm⁻³, based on a room-temperature value[29] of 3.960 and mean thermal expansion coefficients of 9 (respectively 8.3) × 10⁻⁶/°C for c (respectively a) over the range 25–1000 °C,[29] and of 12.7 × 10⁻⁶/°C for both a and c over the interval 1000–2050 °C;[30] for liquid Al₂O₃, among many reported data, the more recent and accepted value[31,32] of 3.01 g cm⁻³ was adopted. Thus the density decrease upon melting, relative to the solid, is 18.94%, in good agreement with a 20.4% volume expansion relative to the liquid, observed for many oxides.[33] These data define a solid–liquid equilibrium line, the gradient of which at the melting point is calculated to be 90.7216 atm K⁻¹, and which, although curved near the triple point, provides an excellent estimate for this latter at its intersec-

Table 5
Calculated [Al$_2$O$_3$] sublimation vapour pressures at some temperatures

T (°C) + 0.15	$p_{[Al_2O_3]}$ (atm)
1427	1.91×10^{-9}
1627	2.30×10^{-7}
1727	1.76×10^{-6}
1787	5.44×10^{-6}
1827	1.11×10^{-5}

tion with Eq. (1), yielding 2053.989 K and 4.0565×10^{-4} atm, and thus determining for the solid–vapour equilibrium, the following approximate equation:

$$\text{Ln } p_{[Al_2O_3]} = 25.4364 - \frac{643247}{RT} \tag{2}$$

Some Al$_2$O$_3$ sublimation vapour pressures, in the temperature interval of interest, are listed in Table 5.

4. Discussion

Thermodynamic data of Table 1, joined with standard enthalpies of [O$_2$] dissociation and [H$_2$O] formation, as obtained from Ref. [17], are compared with those from other references in Table 6. As can be seen, agreement with Ref. [34] is satisfactory for the standard heats of formation and excellent for the heats of dissociation; agreement with the heats of reaction of Ref. [35] is less satisfactory, because of arguable thermodynamic evaluations there. It is shown that standard heats of formation have substantial negative temperature coefficients, especially in the lower two temperature intervals, unlike heats of dissociation which are essentially temperature independent, what attests to the high stability of [Al$_2$O], [AlO] and [Al$_2$O$_2$] molecules. The room-temperature dissociation enthalpy of [AlO], reaction (g), corresponds to 5.114 eV/mol, in good agreement with 5.240 eV reported elsewhere.[36] Reactions (k)–(n) are all highly endothermic, with negative temperature coefficients.

Substituting log $p_{[CO]}$ in Table 2 with the corresponding equations of Table 3 results in pressures that can be written as

$$\text{Ln } p_{[Al_xO_y],\text{limit}} = H - \frac{F}{RT} \tag{3}$$

where, using the notations of Tables 2 and 3, $H = (2A + aC)/2bR$ is a positive constant and $F = [(aD + 2B)/2b]$, also > 0, is the activation energy necessary to form each Al-containing gaseous species by volatilisation from the stable precursors of the Al$_2$O$_3$–Al$_4$C$_3$ system. Both of these are listed in Tables 7A and 7B, in the various temperature intervals; an equivalent formulation of Eq. (3) is evidently $p_{[Al_xO_y],\text{limit}} = p_0 \exp(-F/RT)$, with $p_0 = \exp H$. Table 7A shows that regardless of temperature and solid compound, activation energies significantly increase with increasing ratio y/x in [Al$_x$O$_y$], the intervals (kJ mol^{-1}) varying from 330.8–381.8 for [Al], to 432.8–491.4 for [Al$_2$O], 607.8–651.8 and 646.4–719.1 for [AlO] and [Al$_2$O$_2$], and finally 830.0–939.0 for AlO$_2$. According to this sequence, the sublimation enthalpy of Al$_2$O$_3$ should be expected to range between the intervals 607.8–719.1 kJ mol^{-1} and 830.0–939.0 kJ mol^{-1}, and thus to be somewhat larger than the value of 643.25 kJ mol^{-1} established in Eq. (2); thus there may be some uncertainties attached to the vaporization pressures and normal boiling point of Al$_2$O$_3$ used in the above evaluation. Another common trend is the decrease, as temperature increases, of the activation energy necessary to form any given gaseous species from the same precursor (small for [Al], more pronounced for the other species), except for [AlO$_2$] vapourised from Al$_4$O$_4$C, where an increase is observed above T'. The influence of composition is diverse since in the first two temperature intervals, the activation energies of the different vapour species either slightly increase ([Al], [Al$_2$O]), are unchanged ([AlO], [Al$_2$O$_2$]), or slightly decrease ([AlO$_2$]), with increasing Al$_2$O$_3$ mole fraction. Above T', the activation energy to form any vapour species from Al$_2$O$_3$ is always higher than from Al$_4$C$_3$. When oxycarbides have an effect on activation energies, they act as increasers with increasing Al$_2$O$_3$ mole fraction, except for [Al] from Al$_2$OC and [AlO$_2$] from Al$_4$O$_4$C. Below T', the pre-exponential terms of Table 7B (more precisely their

Table 6
Comparison of standard enthalpies of formation, dissociation and reaction

Type of reaction	Species or reaction	Reference, T (°C)	$\Delta_f H°$	This study		
				25–660 °C	660–1227 °C	1227–1827 °C
Standard formation	[AlO]	[34], 25	87,027	80,750	63,138	58,313
	[Al$_2$O]		−138,072	−135,824	−171,367	−182,199
	[Al$_2$O$_2$]		−389,530	−410,600	−444,488	−452,546
Dissociation	(e)[Al$_2$O] → [AlO] + [Al]	[34], 25	548,104 ± 20920	541,572	542,094	542,077
	(f)[AlO] → [Al] + $\frac{1}{2}$ [O$_2$]			244,248	244,451	243,252
	(g)[AlO] → [Al] + [O]		481,160 ± 20920	494,918	497,696	498,103
	(h)[Al$_2$O] → 2 [Al] + $\frac{1}{2}$ [O$_2$]			785,819	786,544	785,329
	(i)[Al$_2$O] → 2[Al] + [O]		1,024,243 ± 29288	1,036,489	1,039,789	1,040,180
	(j)[Al$_2$O$_2$] → 2[AlO]		564,840 ± 20920	572,100	570,765	569,172
Reaction with [H$_2$]	(k)Al$_2$O$_3$ + 3[H$_2$] → 2[Al] + 3[H$_2$O]	[35], 1726.85	1,514,608	1,593,008	1,560,385	1,533,325
	(l)Al$_2$O$_3$ + 2[H$_2$] → [Al$_2$O] + 2[H$_2$O]		941,400	1,051,382	1,022,660	999,130
	(m)Al$_2$O$_3$ + [H$_2$] → 2[AlO] + [H$_2$O]		1,301,224	1,592,900	1,569,122	1,549,089
	(n)Al$_2$O$_3$ + [H$_2$] → [Al$_2$O$_2$] + [H$_2$O]		903,744	1,020,800	998,357	979,917

Table 7A
Activation energies F (kJ mol^{-1}) necessary to form various species by volatilisation in stable system Al_2O_3–Al_4C_3

[Al$_x$O$_y$]	660–1227			1227–T'			T'–1827			
	Al$_4$C$_3$	Al$_4$O$_4$C	Al$_2$O$_3$	Al$_4$C$_3$	Al$_4$O$_4$C	Al$_2$O$_3$	Al$_4$C$_3$	Al$_2$OC	Al$_4$O$_4$C	Al$_2$O$_3$
[Al]	373.4	373.4–381.8	381.8	367.1	367.1–375.4	375.4	367.1	367.1–330.8	330.8–375.4	375.4
[Al$_2$O]	483.1	483.1–491.4	491.4	469.2	469.2–477.5	477.5	432.8	432.8	432.8–477.5	477.5
[AlO]	651.8	651.8	651.8	644.1	644.1	644.1	607.8	607.8–644.1	644.1	644.1
[Al$_2$O$_2$]	732.7	732.7	732.7	719.1	719.1	719.1	646.4	646.4–719.1	719.1	719.1
[AlO$_2$]	911.8	911.8–903.5	903.5	902.7	902.7–894.4	894.4	830.0	830.0–939.0	939.0–894.4	894.4

Table 7B
Values of H for different vapour species and stable precursors in stable system Al_2O_3–Al_4C_3

[Al$_x$O$_y$]	660–1227			1227–T'			T'–1827			
	Al$_4$C$_3$	Al$_4$O$_4$C	Al$_2$O$_3$	Al$_4$C$_3$	Al$_4$O$_4$C	Al$_2$O$_3$	Al$_4$C$_3$	Al$_2$OC	Al$_4$O$_4$C	Al$_2$O$_3$
[Al]	16.7178	16.7178–16.7181	16.7183	16.2136	16.2136	16.2136	16.2136	16.2136–14.0124	14.0124–16.2136	16.2136
[Al$_2$O]	23.2281	23.2281–23.2277	23.2288	22.1161	22.1161	22.1161	19.9149	19.9149	19.9149–22.1161	22.1161
[AlO]	21.6703	21.6703	21.6705	21.0576	21.0576	21.6705	18.8564	18.8564–21.0576	21.0576	21.0576
[Al$_2$O$_2$]	22.9973	22.9973	22.9977	21.9066	21.9066	22.9977	17.5041	17.5041–21.9066	21.9066	21.9066
[AlO$_2$]	24.7758	24.7758–24.7754	24.7756	24.0439	24.0439	24.7756	19.6415	19.6415–26.2451	26.2451–24.0439	24.0439

Napierian logarithm) strongly depend on x and y and are nearly independent of the solid precursor; the only exceptions are for [AlO], [Al$_2$O$_2$] and [AlO$_2$] between 1227 °C and T', where a significant increase is observed. Above T', they vary exactly as do the activation energies.

Actual values displayed in Table 4 represent the decimal logarithms of $p_{[Al_xO_y]}$ and/or $p_{[Al_xO_y],limit}$ in equilibrium with the various stable compounds of the Al_2O_3–Al_4C_3 system, at three temperatures. It immediately appears from this Table and Table 5 that at all temperatures, the major vapour species in reducing conditions, including [Al$_2$O$_3$], are [Al] and [Al$_2$O], as had already been noticed qualitatively several decades ago, e.g. Ref. [37]. It is also clear in Table 4 that in all cases the volatility of Al oxycarbide(s) is intermediate between Al carbide and Al oxide, Al$_2$OC being more volatile than Al$_4$O$_4$C at least as regards the major vapour species. At 786.85 °C (respectively 1286.85 °C), Al$_2$O$_3$ is about 2.5 times (respectively 1.9) less volatile than Al$_4$C$_3$ with respect to [Al] and [Al$_2$O], quite comparable for [AlO] and [Al$_2$O$_2$], and 2.5 times (respectively 1.9) more volatile with respect to [AlO$_2$], while at 1786.85 °C the volatility ratio is approximately 1.65. It can also be seen that, globally speaking, the different vapour species rank in magnitude as do the activation energies for volatilisation, and that except at the highest temperatures, [Al] is more important than [Al$_2$O], what makes it the most likely intermediate in processes which include vapour phase reactions. An important example is the commercial production of AlN powder, by carbonitridation[38] of Al$_2$O$_3$ at 1600 °C, which should preferentially proceed in a two-step mechanism initiated by the formation of [Al] in an equilibrium volatilisation and followed by its spontaneous reaction with [N$_2$], much in the same way as α-Si$_3$N$_4$ is formed[39] from [Si] as RBSN, rather than in a three-step mechanism[22] implicating [Al$_2$O]. At the highest temperatures $p_{[Al_2O]}$ becomes extremely close to $p_{[Al]}$ and may

actually exceed it, as observed at 1826.85 °C where, in equilibrium with Al$_2$OC, i.e. in the range of $\log p_{[CO]}$ values between −0.8828 to −0.7779, $\log p_{[Al]}$ decreases from −2.0902 to −2.1426 whereas $\log p_{[Al_2O]} = -2.1178$, so that an inversion occurs in the predominating vapour species as $\log p_{CO}$ increases from −0.8828 to −0.7779.

Fig. 2 represents the volatility diagram of the stable Al$_2$O$_3$–Al$_4$C$_3$ system at 1786.85 °C and should replace a graph previously issued in Ref. [40]. Limit carbon monoxide pressures are 0.0871 atm for Al$_4$C$_3$ and 0.1535 atm for Al$_2$O$_3$, with an intermediate value of 0.1023 atm delimitating Al oxycarbides; to these correspond, as oxygen pressures, 1.3×10^{-17} atm, 4.1×10^{-17} atm and 1.8×10^{-17} atm, and as carbon dioxide pressures, 1.5×10^{-7} atm, 4.6×10^{-7} atm and 2.05×10^{-7} atm; not shown on the graph are the [Al] and [Al$_2$O$_3$] saturated vapour pressures, which amount to respectively 0.0123 atm, larger than $p_{[Al]}$ and thereby justifying the absence of liquid aluminium in the system, and 5.44×10^{-6} atm, only slightly higher than $p_{[AlO]}$. The gradients of the various straight lines are such that $p_{[Al]}$ is above $p_{[Al_2O]}$ for any value of $\log p_{[CO]}$, and that no crossing is possible for the gaseous species in equilibrium with Al$_4$C$_3$. In turn many intersections may occur on the Al$_2$O$_3$ side, although none is observed for practical values of carbon monoxide pressures, typically not exceeding 1 atm. With a carbon monoxide pressure of 1 atm and at 1786.85 °C, the following pressures (atm) hold at equilibrium with alumina: $p_{[Al]} = 2.00 \times 10^{-4}$; $p_{[Al_2O]} = 7.40 \times 10^{-5}$; $p_{[Al_2O_3]} = 5.44 \times 10^{-6}$; $p_{[AlO]} = 2.54 \times 10^{-8}$; $p_{[Al_2O_2]} = 2.92 \times 10^{-10}$; $p_{[AlO_2]} = 1.48 \times 10^{-12}$ and $p_{[O_2]} = 1.735 \times 10^{-15}$, and all Al-containing vapour species react with oxygen in quantitative equilibria displaced towards [Al$_2$O$_3$], as shown by the reaction constants listed in Table 8. Studying how volatility diagrams vary with temperature, one observes the predominance of [Al$_2$O] on [Al] in their equilibrium with Al$_2$OC above

Table 8
Quantitative vapour phase equilibria between Al-containing species, oxygen and alumina, at 1786.85 °C

Reaction	Equilibrium constant, K_p
$2[AlO_2] = [Al_2O_3] + \frac{1}{2}[O_2]$	1.04×10^{11}
$[Al_2O_2] + \frac{1}{2}[O_2] = [Al_2O_3]$	4.47×10^{11}
$[Al_2O] + [O_2] = [Al_2O_3]$	4.24×10^{13}
$2[AlO] + \frac{1}{2}[O_2] = [Al_2O_3]$	2.03×10^{17}
$2[Al] + \frac{3}{2}[O_2] = [Al_2O_3]$	1.89×10^{24}

1806.65 °C, and that all Al-containing vapour pressures are smaller than 10^{-8} atm below essentially 1000 °C.

5. Conclusion

The thermochemistry of solid–vapour equilibria within the stable Al_2O_3–Al_4C_3 system was modelled. Describing volatilisation of stable compounds into various species evolved into Arrhenius-type equations wherein any pressure is the product of a pre-exponential term and activation energy. Regardless of the precursor, [Al] is characterized by the smallest activation energy and $[AlO_2]$ by the highest; the sublimation enthalpy of Al_2O_3 as calculated from vapourization pressures is 643247 J mol^{-1}. Up to 1806.65 °C, [Al] is the predominant species for any practical pressure of carbon monoxide, and thus the most likely intermediate in processes involving vapour phase reactions; above, $[Al_2O]$ becomes more important than [Al] on a limited range of [CO] pressures (for example between 0.1488 atm and 0.2677 atm, at 1826.85 °C).

Acknowledgements

References

1. Brook, R. J., Advanced ceramic materials: an overview. In *Advanced Ceramic Materials*, ed. R. J. Brook. Pergamon Press, Oxford, 1991, pp. 1–8.
2. Cox, J. H. and Pidgeon, L. M., The X-ray diffraction patterns of aluminium carbide and aluminium oxycarbide Al_4O_4C. *Can. J. Chem.*, 1963, **41**, 1414–1416.
3. Stackelberg, M. V. and Schnorrenberg, E., Aluminium karbid und unterschiedliche karbonitrid phasen. *Z. Phys. Chem.*, 1934, **27**, 37.
4. Jeffrey, G. A. and Slaughter, M., The structure of aluminum tetroxycarbide Al_4O_4C. *Acta Cryst.*, 1963, **16**, 177–184.
5. Lihrmann, J.-M., Thermodynamics of the Al_2O_3–Al_4C_3 system. I. Thermochemical functions of Al oxide, carbide and oxycarbides between 298 and 2100 K. *J. Eur. Ceram. Soc.*, 2007, this issue.
6. Lihrmann, J.-M., Thermodynamics of the Al_2O_3–Al_4C_3 system. II. Free energies of mixing, solid solubilities and activities. *J. Eur. Ceram. Soc.*, 2007, this issue.
7. Amma, E. L. and Jeffrey, G. A., Structure of aluminum oxycarbide Al_2OC: a short-range würtzite super-structure. *J. Chem. Phys.*, 1961, **34**(1), 252–259.
8. Zaretskaya, G. M., Eidel'shtein, F. I. and Sokhor, M. I., Aluminum monooxycarbide in oxysulfide slag. *Izv. Akad. Nauk. SSSR, Neorg. Mater.*, 1972, **8**(1), 84–87.
9. Yokokawa, H., Dokiya, M., Fujishige, M., Kameyama, T., Ujiie, S. and Fukuda, K., X-ray powder diffraction data for two hexagonal aluminium monoxycarbide phases. *J. Am. Ceram. Soc.*, 1982, **65**(3), 40–41.
10. Ryabkov, Yu. I. and Grass, V. E., Thermal stability of aluminum oxycarbides. *Russ. J. Phys. Chem.*, 2004, **74**(7), 989–992.
11. Ryabkov, Yu. I., Grass, V. E. and Sitnikov, P. A., Thermodynamics of the Al–C–O system. *Russ. J. Phys. Chem.*, 2002, **72**, 165.
12. Cutler, I. B., Miller, P. D., Rafaniello, W., Park, H. K., Thomson, D. P. and Jack, K. H., New materials in the Si–C–Al–O–N and related systems. *Nature*, 1978, **275**, 434–435.
13. Lihrmann, J.-M., Zambetakis, T. and Daire, M., High temperature behavior of the aluminum oxycarbide Al_2OC in the system Al_2O_3–Al_4C_3 and with additions of aluminum nitride. *J. Am. Ceram. Soc.*, 1989, **72**(9), 1704–1709.
14. Moissan, H., Réduction de l'alumine par le charbon. *C.R. Séances Acad. Sci.*, 1894, **119**, 935–937.
15. Drowart, J., De Maria, G., Burns, R. P. and Inghram, M. G., Thermodynamic study of Al_2O_3 using a mass spectrometer. *J. Chem. Phys.*, 1960, **32**(5), 1366–1372.
16. Walsh, A. D., Theoretical models of some gaseous molecules. *J. Chem. Soc.*, 1953, 2266.
17. JANAF, *Thermochemical Tables (2nd ed.)*. National Bureau of Standards (NIST), Gaithersburg, MD, USA, 1971.
18. Morfopoulos, V. C. P., Analysis of the thermodynamics of the Al–C–O system in the temperature range 1000 to 1800 K. *Can. Metal. Quart.*, 1964, **3**(1), 95–116.
19. Worrell, W. L., Carbothermal reduction of alumina. *Can. Metal. Quart.*, 1965, **4**(1), 87–95.
20. Kozhenikov, G. N., Vodop'yanov, A. G., Ovchinnikova, L. A. and Shibaeva, S. V., Reaction of monovalent aluminum oxide with silicon carbide. *Izv. Akad. Nauk. SSSR Met.*, 1976, **6**, 76–79.
21. Vodop'yanov, A. G., Serebryakova, A. V. and Kozhenikov, G. N., Kinetics and mechanism of interaction of Al_2O_3 with carbon. *Izv. Akad. Nauk.SSSR, Met.*, 1982, **1**, 43–47.
22. Chen, H. K., Lin, C. I. and Lee, C., Kinetics of the reduction of carbon/alumina powder mixture in a flowing N_2 stream. *J. Am. Ceram. Soc.*, 1994, **77**(7), 1753–1756.
23. Medvedev, V. A., Reactions with aluminium oxide. *Zhur. Fiz. Khim.*, 1958, **32**, 1690.
24. Gadalla, A., Elmasry, M. and Kongkachuichay, P., High temperature reactions within SiC–Al_2O_3 composites. *J. Mater. Res.*, 1992, **7**(9), 2585–2592.
25. Hendry, A., Silicon nitride ceramics. In *Structural Ceramics: Processing, Microstructure and Properties*, ed. J. J. Bentzen *et al.* Riso National Laboratory, Roskilde (Danemark), 1990, pp. 27–38.
26. Lou, V. L. K., Mitchell, T. E. and Heuer, A. H., Review—graphical displays of the thermodynamics of high temperature gas–solid reactions and their application to oxidation of metals and evaporation of oxides. *J. Am. Ceram. Soc.*, 1985, **68**(2), 49–58.
27. Ceralox, *High Purity Aluminum Oxide Data*. Ceralox Inc., Tucson AZ, USA, 2003.
28. Lide, D. R. and Frederikse, H. P. R., *Handbook of Chemistry and Physics (76th ed.)*. CRC Press, 1995–1996, pp. 6–127.
29. Riley, F. L., Aluminum oxide. In *Advanced Ceramic Materials*, ed. R. J. Brook. Pergamon Press, Oxford, 1991, p. 11.
30. Kingery, W. D., Bowen, H. K. and Uhlmann, D. R., *Introduction to Ceramics (2nd ed.)*. John Wiley & Sons, New York, 1976, p. 593.
31. Rasmussen, J. J. and Nelson, R. P., Surface tension and density of molten Al_2O_3. *J. Am. Ceram. Soc.*, 1971, **54**(8), 398–401.
32. Turkdogan, E. T., *Physico-chemical properties of molten slags and 'glasses'.*. The Metals Society, London, 1983.

33. Kingery, W. D., Surface tension of some liquid oxides and their temperature coefficients. *J. Am. Ceram. Soc.*, 1959, **42**(1), 6–8.

34. Drowart, J., De Maria, G. and Inghram, M. G., Volatilisation study of Al_2O_3. *J. Chem. Phys.*, 1960, **32**(5), 1372–1377.

35. Kuczinsky, G. C. and Ready, D. W., Sublimation of aluminum oxide. *J. Am. Ceram. Soc.*, 1966, **49**(1), 26–29.

36. Mc Donald, J. K. and Innes, K. K., Study of gaseous Al-containing molecules. *J. Mol. Spectrosc.*, 1969, **32**, 501.

37. Brewer, L. and Searcy, A. W., The gaseous species of the $Al–Al_2O_3$ system. *J. Am. Chem. Soc.*, 1951, **73**, 5308–5314.

38. Kranzmann, A., Aluminium nitride. In *Advanced Ceramic Materials*, ed. R. J. Brook. Pergamon Press, Oxford, 1991, pp. 8–9.

39. Moulson, A. J., Review—reaction-bonded silicon nitride: its formation and properties. *J. Mater. Sci.*, 1979, **14**(5), 1017–1051.

40. Lihrmann, J.-M., Tirlocq, J., Descamps, P. and Cambier, F., Thermodynamics of the Al–C–O system and properties of $SiC–AlN–Al_2OC$ composites. *J. Eur. Ceram. Soc.*, 1999, **19**, 2781–2787.